

Structural and Electrochemical Properties of $\text{Li}[\text{Cr}_{0.29}\text{Li}_{0.24}\text{Mn}_{0.47}]\text{O}_2$ Nanocomposite Electrode for Lithium-ion Batteries

Chan-Woo Park and Jaekook Kim*

Department of Materials Science and Engineering, Chonnam National University, Gwangju 500-757, Korea

(Received May 17, 2006; CL-060586; E-mail: jaekook@chonnam.ac.kr)

$\text{Li}[\text{Cr}_{0.29}\text{Li}_{0.24}\text{Mn}_{0.47}]\text{O}_2$ with nanocomposite structures was synthesized by a solution method with subsequent quenching. The crystalline structure was investigated by X-ray diffraction (Rietveld refinement), electron diffraction, and HRTEM. According to coindexed electron diffraction patterns and HRTEM images, $\text{Li}[\text{Cr}_{0.29}\text{Li}_{0.24}\text{Mn}_{0.47}]\text{O}_2$ was found to be nanocomposite powders indexed in monoclinic and hexagonal structures. The nanocomposite cathode prevented spinel-like structural transformation during cycling and delivered a good reversible capacity of about 195 mA h/g.

Manganese-based electrode materials still have been widely studied for their low cost, nontoxicity, and relative stable thermal properties, although LiMn_2O_4 suffers from capacity fading due to the dissolution of manganese and Jahn–Teller distortion, and layered LiMnO_2 transforms into a spinel structure during the lithium insertion/extraction process owing to cation migration.^{1–3} Recently, derivative of layered manganese oxides such as substituted $\text{LiM}_x\text{Mn}_{1-x}\text{O}_2$ and solid solutions or nanocomposite $\text{Li}_2\text{MnO}_3\text{--LiMO}_2$ ($\text{M} = \text{Ni}, \text{Co}, \text{or Fe}$)^{4–8} have been investigated, in order to obtain cathodes with prolonged structural integrities and enhanced electrochemical performance. The synthesis of composite $x\text{Li}_2\text{MnO}_3 \cdot (1-x)\text{LiMn}_{0.5}\text{Ni}_{0.5}\text{O}_2$ electrodes has been reported.⁹ According to analyses conducted by powder X-ray diffraction (XRD), high-resolution transmission electron microscopy (HRTEM), X-ray absorption spectroscopy (XAS), and nuclear magnetic resonance (NMR) spectroscopy, lithium-saturated solid solutions or nanocomposite $\text{Li}_2\text{MnO}_3\text{--LiMO}_2$ structures comprise nanometer regions with Li_2MnO_3 - and LiMO_2 -like features, confirming the composite character of these materials. The objective of the present work is to reveal the reason for high capacity and good cyclability of $\text{Li}[\text{Cr}_{0.29}\text{Li}_{0.24}\text{Mn}_{0.47}]\text{O}_2$ synthesized using a solution method with subsequent quenching process. In particular, we focus on characterizing the nanoscale local structures with respect to electrochemical behavior of nanocomposite electrode materials.

$\text{Li}[\text{Cr}_{0.29}\text{Li}_{0.24}\text{Mn}_{0.47}]\text{O}_2$ material was prepared by mixing appropriate molar ratios of chromium acetate, manganese acetate, and lithium hydroxide. A 100 mL of aqueous solution of $\text{LiOH} \cdot \text{H}_2\text{O}$ was slowly dripped into a 100 mL of predissolved solution of the transition-metal acetates. Stirring was continued for 24 h to ensure a homogeneous reaction. The solution was dried in air until a gel is obtained. The gel thus obtained was heated initially in an oven at 110 °C for 6 h, and then ground and heated at 600 °C for 3 h. Finally, the powders were fired at 900 °C for 12 h and quenched using two copper plates. The prepared samples were washed with distilled water to remove Li_2CrO_4 and dried in vacuum at 100 °C.¹⁰ The elemental composition of the prepared cathode powders was determined by inductively coupled plasma (ICP) analysis. A detailed analysis

of the crystallinity was conducted by examining the TEM spot patterns, and TEM images were collected under an accelerating voltage of 200 keV. An electrolyte consisting of a 1 M solution of LiPF_6 in ethylene carbonate (EC) and dimethyl carbonate (DMC) (1:1, v/v) was used and the cells were assembled in an argon-filled glove box.

The ICP result of $\text{Li}[\text{Cr}_{0.29}\text{Li}_{0.24}\text{Mn}_{0.47}]\text{O}_2$ shows that the chromium content is decreased when the stoichiometrically synthesized compounds of $\text{Li}[\text{Cr}_{0.5}\text{Li}_{0.166}\text{Mn}_{0.33}]\text{O}_2$ is washed with distilled water. This fact is confirmed with the XRD patterns of the samples recorded before and after the elimination of Li_2CrO_4 as shown in Figure 1. The Li_2CrO_4 peaks appeared in the XRD pattern (Figure 1a) of the sample before the washing disappeared in that of the sample after washing it with distilled water (Figure 1b).

Figure 2 shows the electron diffraction patterns obtained from $\text{Li}[\text{Cr}_{0.29}\text{Li}_{0.24}\text{Mn}_{0.47}]\text{O}_2$ together with monoclinic Li_2MnO_3 and rhombohedral LiCrO_2 . The diffraction patterns shown in Figures 2a and 2b were indexed based on the monoclinic structure in the [101] zone and that shown in Figure 2c coincided with the rhombohedral in the $[1\bar{1}\bar{1}]$ zone. The corresponding schematic presentations of atomic structures are given in Figure 3a, which shows the Li_2MnO_3 structure ordered in the [101] zone and in Figure 3b, which shows the layered LiCrO_2 structure ordered in the $[1\bar{1}\bar{1}]$ zone, respectively.

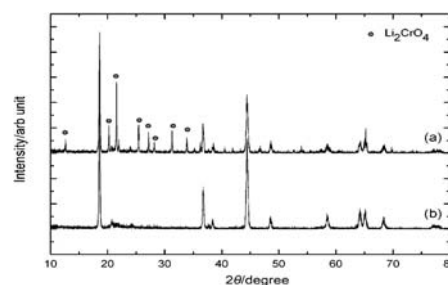


Figure 1. X-ray diffraction patterns of (a) before washing and (b) after washing of $\text{Li}[\text{Cr}_{0.29}\text{Li}_{0.24}\text{Mn}_{0.47}]\text{O}_2$ sample.

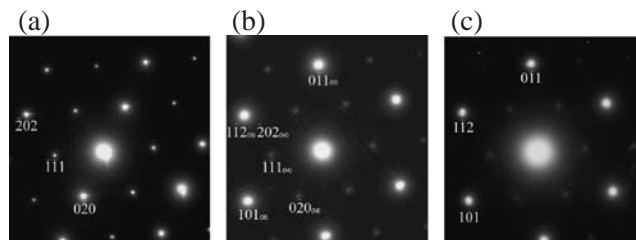


Figure 2. The electron diffraction patterns of (a) monoclinic Li_2MnO_3 , (b) $\text{Li}[\text{Cr}_{0.29}\text{Li}_{0.24}\text{Mn}_{0.47}]\text{O}_2$, and (c) rhombohedral LiCrO_2 .

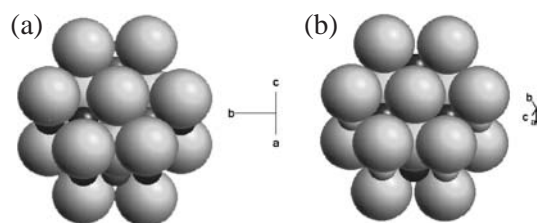


Figure 3. Schematic representations of (a) monoclinic structure ([101] zone) and (b) rhombohedral structure ([111] zone).

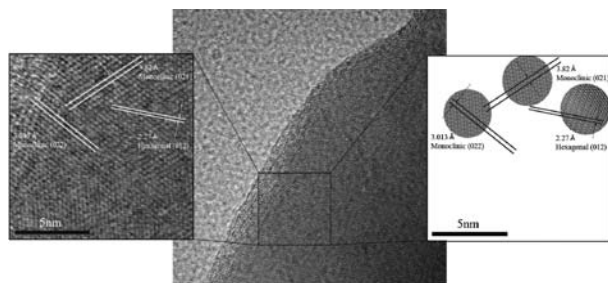


Figure 4. HRTEM images of nanocomposite electrode material.

Interestingly, the faint spots in Figure 2b were indexed based on the monoclinic structure ordered in the [101] zone. It suggests that Li_2MnO_3 ordered in the [101] zone coexist with the layered LiCrO_2 ordered in the [111] zone in nanocomposite $\text{Li}[\text{Cr}_{0.29}\text{Li}_{0.24}\text{Mn}_{0.47}]\text{O}_2$ sample. The uncertainly defined crystal structure obtained using X-ray diffraction was clearly classified using the electron diffraction patterns, since the electron diffraction patterns of the monoclinic and hexagonal structures are clearly distinguishable, even though both have layered structure. The characterization of the crystal structure would also be able to be confirmed by comparing the electron diffraction patterns of another zone axis directions such as monoclinic [110] and rhombohedral [120].

With respect to the XRD and electron diffraction results, the formation of the nanocomposite in $\text{Li}[\text{Cr}_{0.29}\text{Li}_{0.24}\text{Mn}_{0.47}]\text{O}_2$ sample was verified by examining the HRTEM images. Figure 4 shows that throughout the primary particles, the monoclinic and rhombohedral phases are coexisted by forming a nanodomains. This can be explained by the fact that the selectively surrounding lithium around manganese might cause a difference in strength of the bonds between transition metal and oxygen layers; hence, the distance between the planes will be varied. It suggests that progressed separations with $[\text{Li}_{1/3}\text{Mn}_{2/3}]$ cluster and Cr induce the divided phases as monoclinic and rhombohedral crystal structures in a particle. Figure 5 shows the discharge curves of $\text{Li}[\text{Cr}_{0.29}\text{Li}_{0.24}\text{Mn}_{0.47}]\text{O}_2$ cycled between 2.4 and 4.7 V with a current density of 11.98 mA/g. In general, it is believed that only chromium is the redox active species cycling between Cr^{3+} and Cr^{6+} .¹¹ This would mean that oxidation state of manganese is maintained as +4 and the Mn^{4+} ion with surrounding Li works inert in Li_2MnO_3 -like framework. Although it is assumed that the manganese-based electrode could be transformed to spinel-like structure after extended cycling, the electrochemical property of $\text{Li}[\text{Cr}_{0.29}\text{Li}_{0.24}\text{Mn}_{0.47}]\text{O}_2$ shows a good capacity retention compared with results from

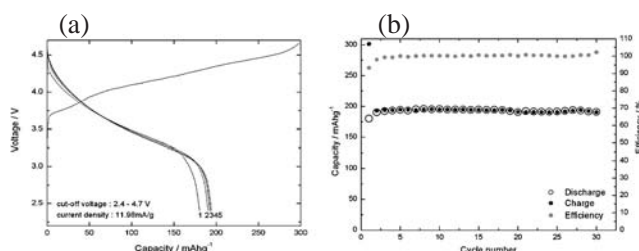


Figure 5. Discharge curves and capacity retention of $\text{Li}[\text{Cr}_{0.29}\text{Li}_{0.24}\text{Mn}_{0.47}]\text{O}_2$ between 2.4 and 4.7 V.

other layered manganese-based electrodes which suffer from transformation-induced Jahn–Teller distortion. It is assumed that nanodomains of both of electrochemically inert LiCrO_2 and Li_2MnO_3 -like phases in a primary particle act as a framework sharing the oxygen lattices so that it allows circumventing the problems.

$\text{Li}[\text{Cr}_{0.29}\text{Li}_{0.24}\text{Mn}_{0.47}]\text{O}_2$ was synthesized by a solution method and subsequent quenching process. It is indexed based on the rhombohedral structure O3-LiCoO_2 with broad super-structure peaks in the scattering angle range between 20 and 35°. By coindexing the electron diffraction pattern, the samples were found to be composed of nanocomposite phases. From the HRTEM images, it is clear that $\text{Li}[\text{Cr}_{0.29}\text{Li}_{0.24}\text{Mn}_{0.47}]\text{O}_2$ is composed of nanocomposite domains of rhombohedral and monoclinic phases. The nanocomposite $\text{Li}[\text{Cr}_{0.29}\text{Li}_{0.24}\text{Mn}_{0.47}]\text{O}_2$ delivered a good reversible capacity of 195 mA h/g between 2.4 and 4.7 V. The nanocomposite electrode with mixed monoclinic and hexagonal structure sharing oxygen lattices is found to be preserved its structural integrity through extended cycles.

This work was supported by the Core Technology Development Program of the Ministry of Commerce, Industry and Energy (MOCIE).

References

- 1 S. J. Wen, T. J. Richardson, L. Ma, K. A. Striebel, P. N. Ross, E. J. Cairns, *J. Electrochem. Soc.* **1996**, *143*, L136.
- 2 M. M. Thackeray, Y. Shao-Horn, A. J. Kahaian, K. D. Kepler, E. Skinner, J. T. Vaughey, S. J. Hackney, *Electrochem. Solid-State Lett.* **1998**, *1*, 7.
- 3 L. Croguennec, P. Deniard, R. Brec, *J. Electrochem. Soc.* **1997**, *144*, 3323.
- 4 M. H. Rossouw, M. M. Thackeray, *Mater. Res. Bull.* **1991**, *26*, 2864.
- 5 K. Numata, S. Yamanaka, *Solid State Ionics* **1999**, *118*, 117.
- 6 Z. Lu, L. Y. Beaulieu, R. A. Donabarger, C. L. Thomas, J. R. Dahn, *J. Electrochem. Soc.* **2002**, *149*, A778.
- 7 C. Storey, I. Kargina, Y. Grincourt, I. J. Davidson, Y. Yoo, D. Y. Seung, *J. Power Sources* **2001**, *97–98*, 541.
- 8 Y. Grincourt, C. Storey, I. J. Davidson, *J. Power Sources* **2001**, *97–98*, 711.
- 9 C. Storey, I. Kargina, Y. Grincourt, I. J. Davidson, Y. Yoo, D. Y. Seung, Proceedings of the 10th International Meeting on Lithium Batteries, Como, Italy, May 28–June 2, **2000**, Abstr., No. 234.
- 10 Z. P. Guo, S. Zhong, G. X. Wang, G. Walter, H. K. Liu, S. X. Dou, *J. Electrochem. Soc.* **2002**, *149*, A792.
- 11 B. Ammundsen, J. Paulsen, *Adv. Mater.* **2001**, *13*, 943.